ENHANCED ANALYSIS OF UTERINE ACTIVTY USING SURFACE ELECTROMYOGRAPHY

A. Herzog, L. Reicke, M. Kröger
Institute of Dynamics and Vibration Research, Leibniz University Hannover, Germany

C. Sohn, H. Maul
Obstetrics and Gynecology, UniversityHospital Heidelberg, Germany

Keywords: Uterine, electromyography, pulse detection, stochastic analysis, Karhunen-Loève, principal component.

Abstract: This contribution presents a new approach for the enhanced analysis of uterine surface electromyography (EMG). First, a pulse detection separates the pulses, which contain the essential information about the uterine contractibility, from the flat line sections during relaxation. The functionality of this semi-automatic algorithm is controlled by two comprehensible parameters. Subsequently, the mean frequency, which serves as a criterion for imminent delivery, is evaluated from the extracted pulses. Although the pulse detection reduces the deviation of the mean frequency significantly, the results are still sensitive to parameter variations in the pulse detection. A stochastic analysis based on the Karhunen-Loève transform (KLT) derives generalised patterns, the eigenforms, from the pulse ensemble. The mean frequency of the first eigenform is less sensitive to parameter variations. Additionally, the correlation between the eigenforms of the left and right surface electrode can serve as a criterion for the measurement's quality.

1 INTRODUCTION

Even in modern obstetrics, the point of delivery cannot be precisely predicted. Although the majority of pregnancies passes without any complications, the significance of an enhanced analysis of uterine activity arises from the diagnosis of preterm labor as well as the treatment of delayed delivery.

The uterine muscle (myometrium), which has maintained a quiescent state during the majority of pregnancy, is prepared for labor by local contractions. These contractions, called training labors, improve the synchronisation between the single muscle cells in order to obtain a defined contraction sequence during delivery. Therefore, the identification of imminent labor requires an elaborate analysis and interpretation of this preparatory phase.

Several methods for the evaluation of uterine contractibility are commonly used: TOCO, IUPC and EMG. Uterine contractions cause variations in the abdomen's contour, which can be detected by pressure sensors. Due to the indirect measurement, this so-called external tocodynamometry (TOCO) is not sensitive and reliable enough. A more reliable approach consists of measuring the uterine's internal pressure (intrauterine pressure catheter, IUPC). The surface electromyography (EMG) combines the non-invasiveness property of TOCO with a sensitivity similar to that of the IUPC (Maul et al., 2004). The muscular activity is accompanied by variations of the electric potential at the neuromuscular junction between nerve and muscle cells. This potential can be picked up directly by needle electrodes and range from $-70\,\mathrm{mV}$ (relaxation) up to $+30\,\mathrm{mV}$ during contraction. In case of surface electrodes, the voltage has to be transmitted via the tissue to the skin, yielding to lower peak values as well as deformations in the time history of the voltage signal. For the measurement of the uterine contractions two surface electrodes are used. They are located on the right and left side of the abdomen. The time-history of a single electromyogram (EMG)-signal is displayed in Figure 1 above. The pulses, which belong to uterine contractions, are separated by flat line sections. Up to now, the frequency characteristics have been derived from large sections of its time history by means of the Fourier transform. Based on the assumption that ongoing synchronisation leads to an increase of the pulse's attack

Herzog A., Reicke L., Kröger M., Sohn C. and Maul H. (2008).
ENHANCED ANALYSIS OF UTERINE ACTIVTY USING SURFACE ELECTROMYOGRAPHY.
In *Proceedings of the First International Conference on Bio-inspired Systems and Signal Processing*, pages 377-384
DOI: 10.5220/0001062903770384

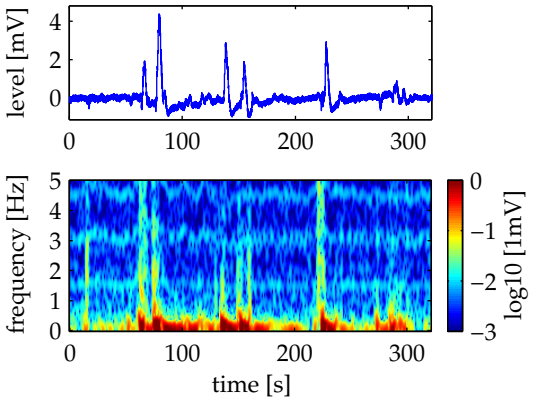

Figure 1: Surface Electromyogram: Time history (above) and its short-time Fourier transform (below).

and decay slope, the mean frequency of the calculated spectrum serves as a criterion to judge imminent delivery.

But a detailed analysis in the time-frequency domain reveals a strongly varying frequency content. This analysis is done by a discrete short-time Fourier transform (STFT) based on a Hann-Window 5 s long. An additional zero-padding and a logarithmic scaling of the resulting amplitude-coefficients unveils all the significant details. An introduction into the time-frequency transforms can be found in (Mertins, 1999), practical aspects are discussed e.g. in (Reicke et al., 2006).

The logarithmic representation of the STFT coefficients in Figure 1 does not only show the broad frequency content of the pulses, it even unveils the heart beat of the foetus at 1.6 Hz as well as its harmonics. Due to the fact that the pulses rather than the flat line sections contain the information about the uterine contractibility, the authors suggest an enhanced analysis which is restricted to the EMG-pulses. This new approach is supported by Figure 2. The diagram on the top shows the instantaneous mean frequency

$$f_{\mathrm{m}}(t) = \int_0^\infty f \cdot \frac{|X_{\mathrm{STFT}}(f,t)|^2}{||X_{\mathrm{STFT}}(t)||^2}\,\mathrm{d}f \qquad (1)$$

derived from the amplitude coefficients $X_{\mathrm{STFT}}(f,t)$ of the STFT. The norm $||X_{\mathrm{STFT}}(t)||$ denotes the instantaneous energy $\int |X_{\mathrm{STFT}}(f,t)^2|\,\mathrm{d}f$ of the STFT. The red line represents the level of the original EMG-signal. The lower diagram shows the evolution of the mean frequency's standard deviation

$$\sigma_f(t) = \sqrt{\int_0^\infty (f - f_{\mathrm{m}})^2 \cdot \frac{|X_{\mathrm{STFT}}(f,t)|^2}{||X_{\mathrm{STFT}}(t)||^2}\,\mathrm{d}f} \qquad (2)$$

over time. It underlines that a reliable estimation of the mean frequency is restricted to the pulses. Only in these time intervals, the standard deviation is less than 3 Hz.

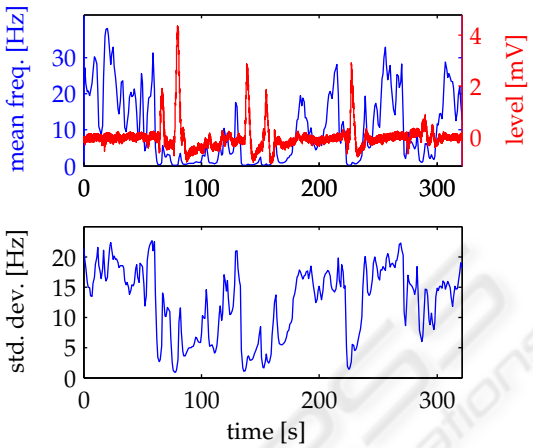

Figure 2: Instantaneous mean frequency (above) and its standard deviation (below) of the signal shown in Fig. 1.

As only the pulses contain the relevant information, it is convenient to analyse the pulses without the intervals of relaxation. This contribution presents a semi-automatic pulse detection, which extracts the pulses out of the measured EMG-signal. The expression *semi-automatic* underlines that the operation is controlled by the physician, whereas the algorithm undertakes the time-consuming and exhausting work of scanning through the signal searching for pulses. Additionally, the use of surface electrodes causes deformations of the pulse shape. Therefore, the pulses are processed by a stochastic method based on the Karhunen-Loève transform to evaluate a generalised pattern.

2 PULSE DETECTION

2.1 Conditioning

The surface-EMG signals are distorted by noise and a low frequency drift. A low-pass filter, which rejects frequencies higher than 7.5 Hz, is applied to attenuate the noise. The low frequency drift is reduced by a high-pass filter with a cut-off frequency of 0.1 Hz and a transition band of 0.2 Hz. Both are implemented as finite impulse response (FIR) filters based on a Kaiser window design (Oppenheim and Schafer, 1999). An additional noise-reduction is achieved by the pulse detection: the flat line intervals, which are characterised by a low signal-to-noise ratio, are excluded from the further analysis.

2.2 Pulse Detection

The pulse detection extracts those parts of the signal which contain the relevant information about the uterine contractibility. The localisation of the pulses is done regarding the magnitude of the signal. First, the global maximum and the mean value of the signal's magnitude as an approximation of the noise level are determined. All local peaks in the range between these two values can be considered as potential pulse centres. But only pulses whose peak values largely exceed the noise limit offer a sufficient signal-to-noise ratio. Therefore, the first parameter of the pulse detection, the *level value*, is introduced. This value determines the percentage of the range between noise level and global maximum which is added to the noise level in order to define the lower level limit. If the level value is chosen equal to zero, the lower level limit is identical to the noise level. Hence, any peak value higher than the noise level is considered as a pulse centre. In case of a level value equal to "1", the lower level limit reaches the global maximum and any peak except for the global maximum will be rejected. Figure 3 shows a particular lower level limit which corresponds to a level value of 0.3.

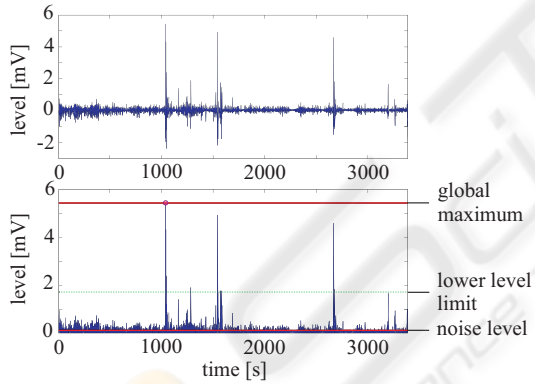

Figure 3: EMG-signal (above) and its magnitude with global maximum, noise level and a particular level value.

After the localisation of the pulse centres in the signal, the initial and end point of each pulse are determined. The pulse detection is based on the assumption that a pulse begins and ends at roots. Therefore, any low frequent drift has to be removed (cp. 2.1) before the execution of the pulse detection algorithm. Starting with the pulse centre, the adjoining roots temporary describe the initial and end points. In the following, this part of the pulse between these two roots is called the inner pulse. If these points were finally considered as the pulse's initial and end points, adjacent over- and undershoots, which might belong to the pulse and therefore contain valuable information, would not be extracted. Hence, the surroundings of the inner pulse have to be taken into consideration.

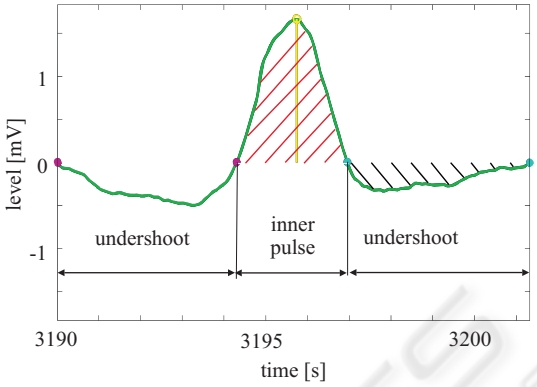

Figure 4: Evaluation of inner and outer area.

Figure 4 displays a pulse with a preceding and subsequent undershoot. To determine whether these undershoots are part of the pulse, the roots before and after the temporary initial and end points are considered. For example, the temporary end point and the root located on its right enclose the subsequent undershoot. Now, the area of the undershoot is calculated and related to the area of the inner pulse. In Figure 4, the area of the undershoot ("outer area") and the inner pulse ("inner area") are hatched in black and red, respectively. If the ratio of the outer and inner area exceeds a given value, the corresponding undershoot belongs to the pulse. If the right undershoot in Figure 4 fulfils this area criterion, the inner pulse is expanded by the right undershoot and the temporary end point is shifted by one root to the right.

This given value is called the *area value* and can be chosen anywhere between "0", which connects any adjacent undershoot to the inner pulse, and "1". In case of an area value equal to "1", only undershoots exhibiting an area greater than the inner area are attached to the pulse. The same procedure is done with the undershoot on the left. This algorithm goes on in both directions until the area of the current over- or undershoot is less than that of the original inner pulse. In this case, the temporary root becomes the final root, which borders the pulse to one side. As soon as the left and right final roots are determined, the pulse can be extracted from the signal. The detection of the next pulses follows the same algorithm. In order to avoid overlapping of closely neighbouring pulses, the extracted pulse data are replaced by zeros.

The level value influences the quantity of detected pulses. The lower the level value, the more peaks of the signal are regarded as pulse centres. The area value controls the lengths of the pulses. The greater the area value, the less over- and undershoots belong to the inner pulse and therefore the less pulses are

lengthened beyond their inner pulse. However, the area value has an influence on the quantity of the pulses, too. If the area value is very low, the pulses extracted from the signal are so long that less pulses can be detected in the remaining signal parts.

2.3 Characteristic Values

The pulse detection scans through the signal and cuts out single time histories belonging to those pulses whose shapes match the pattern specified by the level and area value. The extracted pulses are described in the time domain by their peak values and lengths. Additionally, each pulse is analysed in the frequency domain by the discrete Fourier transform (DFT). Contrary to the short-time Fourier transform $X_{\mathrm{STFT}}(f,t)$ of the entire signal, the spectrum $X_{\mathrm{pulse}}(f)$ of an individual pulse is not time-dependent. Hence, each pulse is characterised by two values in the frequency domain, the mean frequency f_m and the variance σ_f^2.

Based on a measured EMG-signal, Figure 5 shows the characteristic values of those pulses that fulfill a level value equal to "0.3", i.e. 30 % of the global maximum, and an area value of "0.4". In the diagrams, the horizontal line denotes the arithmetic mean. The third diagram exhibits a strong variation in the pulse length. Particularly, the 2nd and 4th pulse length strongly deviate from the mean of ≈ 650 samples. The 2nd pulse's mean frequency f_m largely exceeds the mean of ≈ 0.16 Hz. The reason may be the short duration of ≈ 200 Samples, which also increases the variance σ_f^2.

In order to demonstrate the influence of the two parameters *level value* and *area value* on the number, length and mean frequency of the pulses extracted from the EMG-signal, the results of five different pairs, shown in Table 1, are compared in Figures 6, 7 and 8.

Table 1: Pairs of parameters used for pulse detection.

parameter settings	level value	area value
E1	0.05	0.1
E2	0.1	0.1
E3	0.1	0.3
E4	0.3	0.4
E5	0.3	0.7

For each pair, denoted with E1 up to E5, the left and right bars represent the left and right channel of the electromyogram, respectively. With increasing level value, the number of pulses decreases because pulses with lower peak values are now rejected. A comparison between pair E2 and E3 as well as E4 and E5 unveils the influence of the area value on the length and number of pulses. An increasing area value leads to a shorter maximum pulse length. On the other hand, a higher level value increases the minimum pulse length because the pulses with low peak values, which are obviously shorter, are not considered anymore. As it is mentioned in 2.2, a more restrictive area value can resolve and separate closely neighbouring pulses into two individual pulse shapes.

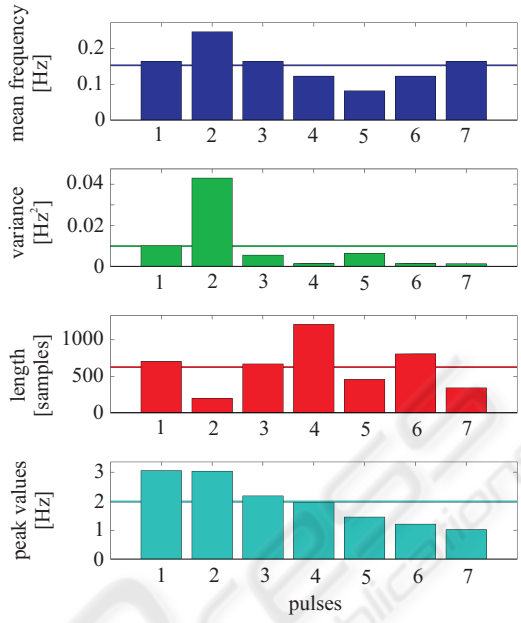

Figure 5: Characteristic values of a pulse ensemble cut out from a measured EMG-signal.

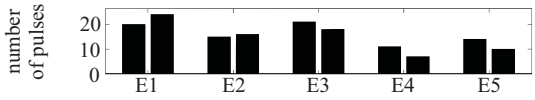

Figure 6: Influence of parameters in Table 1 on number of pulses extracted.

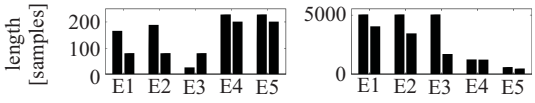

Figure 7: Influence of parameters in Table 1 on minimum and maximum pulse length.

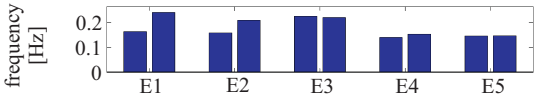

Figure 8: Influence of parameters in Table 1 on mean frequency.

The variation of the pulse length takes effect on the mean frequency, which is shown in Figure 8. It

reveals a strong sensitivity of the mean frequency to the given level and area values. This insufficient uncertainty motivated the authors to improve the analysis by a stochastic signal processing, which is described in the next section. Additionally, a criterion is required to give reliable information about the quality of the signal. A straightforward approach is the consideration of the signal-to-noise ratio, but this will not take into account any correlation between the two channels .

3 STOCHASTIC ANALYSIS

3.1 Karhunen-Loève Transform

The electric potential, which occurs at a neuromuscular junction, is transmitted via a quite complex electric network to the two electrodes at the abdomen's surface. This leads to an amplitude attenuation of $\approx -20\,\mathrm{dB}$ and deformations in the pulse shape. In addition, the location of the contraction is randomly distributed over the entire uterine muscle, which implies a random distortion of the EMG-signal with regard to the peak value and pulse shape.

Due to the fact that the measuring time of about 30 min is very short compared to the ongoing pregnancy, a stationary stochastic process is assumed. The individual pulse shapes extracted by the pulse detection are considered as the realisations of this stochastic process. The new approach uses the Karhunen-Loève transform (KLT), also referred to as Principal Component Analysis (PCA), to determine a characteristic pulse shape out of the pulse ensemble.

The Karhunen-Loève transform is a signal-depending decomposition based on the covariance matrix

$$\underline{R}_{\tilde{x}\tilde{x}} = \mathrm{E}\left\{\underline{\tilde{x}}\,\underline{\tilde{x}}^{\mathrm{T}}\right\}, \tag{3}$$

in which $\mathrm{E}\{\ \}$ denotes the statistic expectation and $\tilde{x}$ the stochastic process. The decomposition requires the eigenvectors $\underline{u}$ of the eigenvalue problem

$$\underline{R}_{\tilde{x}\tilde{x}}\,\underline{u} = \lambda\,\underline{u}. \tag{4}$$

The eigenvectors $\underline{u}$ can be regarded as the characteristic shapes of the stochastic process. The eigenvalue λ represents the degree of similarity between the corresponding eigenvector and the individual pulses. In the following, the product of eigenvector and eigenvalue is denoted as *eigenform*. The more similar the individual pulses of the ensemble are to each other, the more dominant becomes the first eigenform. If the ensemble consists of identical pulse shapes, the first eigenvalue will contain the whole variance of the stochastic process, while all other eigenvalues are equal to 0. A brief introduction into the Karhunen-Loève transform is given in (Mertins, 1999), a detailed description can be found in (Jolliffe, 2002).

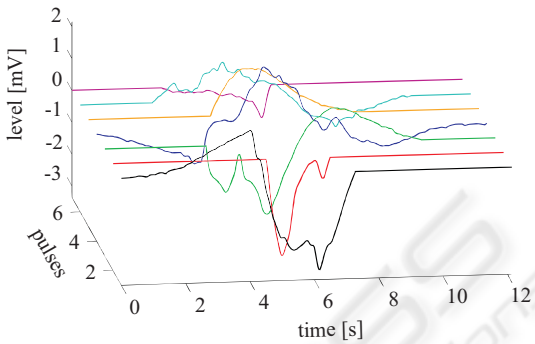

Figure 9: Ensemble of centred pulses.

For the stochastic analysis, a preprocessing of the pulses is necessary. The calculation of the covariance matrix requires an identical length of all the pulse shapes. Therefore, the pulses are centered with regard to their centres of area, followed by padding zeros on both sides to obtain an identical pulse length. The result of this preprocessing is shown in Figure 9, in which the longest pulse, the blue one, specifies the dimension of the covariance matrix. The other pulse shapes are shifted in such a way that all area centres coincide.

The result of the KLT of Figure 9 is displayed in Figure 10: The first and second eigenforms (EF) are dominant and contain $\approx 90\,\%$ of the process' variance. This can be seen from the time history on the left side as well as the loadings on the right. In this context, the loading denotes the normalised variance of the stochastic process.

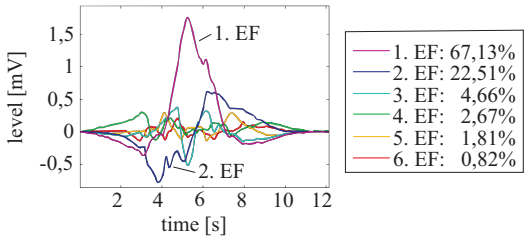

Figure 10: KLT: Eigenforms (left) and loadings (right).

Instead of deriving the mean frequency directly from the pulse ensemble (cp. subsection 2.3), the DFT of the first eigenform yields to a mean frequency which is less sensitive to parameter variations. On top of Figure 11, the global mean frequency, which is evaluated as the arithmetic mean of the individual eigenforms' mean frequencies, is displayed according to the parameter settings shown in Table 1. While

the global mean frequency is susceptible to parameter variations, the mean frequency derived from the first eigenform seems to be less sensitive. Here, research is in progress to confirm this observation.

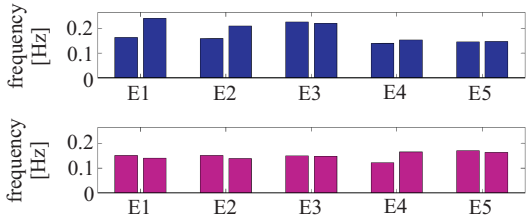

Figure 11: KLT: global mean frequency (above) and mean frequency of the first eigenform (below) for different parameter settings.

The Karhunen-Loève transform does not only extract a characteristic pulse pattern, the first eigenform, out of the pulse ensemble. It can also provide a reliable criterion of the electromyogram's reliability. If the first eigenvalue is dominant, the pattern of the first eigenform is similar to the shapes of the majority of pulses in the ensemble, while the other eigenforms represent the deformations in the pulse shapes.

3.2 Correlation Analysis

So far, the two channels of the electromyogram have been analysed separately. In case of a dominant eigenvalue (see subsection 3.1), the corresponding eigenform characterises the pulse pattern of the individual channel's pulse ensemble very well. Therefore, the correlation between the left and right EMG-channel can be evaluated by regarding their first eigenforms.

Even in case of identical pulse shapes, a time shift between the left and right eigenform can occur. This may be caused by different transmission delays from the neuromuscular junction to the surface electrodes in combination with the centring of the pulses before the KLT is performed.

In order to evaluate the similarities between the left and right eigenform $u_\ell(t)$ and $u_\mathrm{r}(t)$ the cross-correlation function (CCF)

$$R_{u_\ell u_\mathrm{r}}(\tau) = \int_{-\infty}^{\infty} u_\ell(t) \cdot u_\mathrm{r}(t+\tau)\,\mathrm{d}t \qquad (5)$$

is used. If the two eigenforms are of identical shape but shifted to each other, $u_\mathrm{r}(t) = u_\ell(t-\Delta t)$, the CCF resembles an autocorrelation function (ACF) whose maximum value is shifted along the time axis. Due to the fact that an ACF is symmetric to its origin $\tau = 0$, the CCF of two identical but shifted eigenforms is symmetric with regard to the time shift Δt:

$$R_{u_\ell u_\mathrm{r}}(\Delta t - \tau) = R_{u_\ell u_\mathrm{r}}(\Delta t + \tau)\,. \qquad (6)$$

Because the eigenvector's orientation is not specified by Equation 4, the left and right eigenforms can differ in their signs. Therefore, maximum correlation in the CCF appears at its global maximum or minimum. First of all, the time shift of the CCF is determined by its global extremum. Subsequently the CCF is divided into a symmetric

$$R_\mathrm{symm}(\tau) = \frac{R_{u_\ell u_\mathrm{r}}(\Delta t + \tau) + R_{u_\ell u_\mathrm{r}}(\Delta t - \tau)}{2} \qquad (7)$$

and antimetric

$$R_\mathrm{anti}(\tau) = \frac{R_{u_\ell u_\mathrm{r}}(\Delta t + \tau) - R_{u_\ell u_\mathrm{r}}(\Delta t - \tau)}{2} \qquad (8)$$

component. This decomposition is displayed in Figure 12. The extremum is located at ≈ 2000 samples, at which a vertical symmetry axis (dashed line) is drawn. According to Equations 7 and 8 the cross-correlation function (blue line) is decomposed into its symmetric (green line) and antimetric (red line) components.

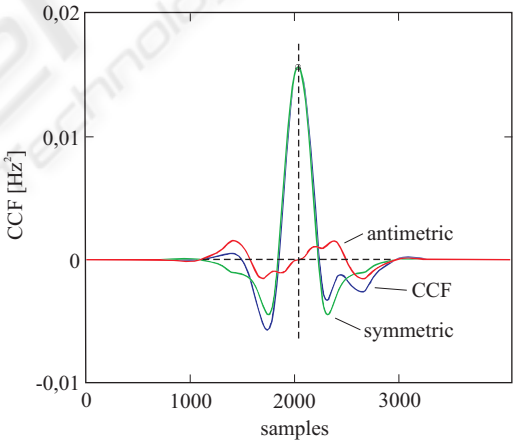

Figure 12: Decomposition of the CCF (blue) at its extremum into a symmetric (green) and antimetric (red) component.

Based on this decomposition a symmetry value

$$C_\mathrm{symm} = 1 - \frac{\int_{-\infty}^{\infty} \left(R_{u_\ell u_\mathrm{r}}(\tau) - R_\mathrm{symm}(\tau)\right)^2 \mathrm{d}\tau}{\int_{-\infty}^{\infty} R^2_{u_\ell u_\mathrm{r}}(\tau)\,\mathrm{d}\tau} \qquad (9)$$

can be specified as the square deviation of the CCF from its symmetric component. In case of full axis symmetry, the symmetric value in Equation 9 reaches "1" or 100 %. The cross-correlation function of the left and right eigenforms for the parameter settings

in Table 1 are displayed in Figure 13. The CCF's oscillations are caused by the under- and overshoots of the EMG-pulses. With an increasing area value, these parts diminish in the pulse shapes and eigenforms. The CCFs are dominated by their symmetric components, which is also confirmed in Table 2 by symmetry values close to 100 %.

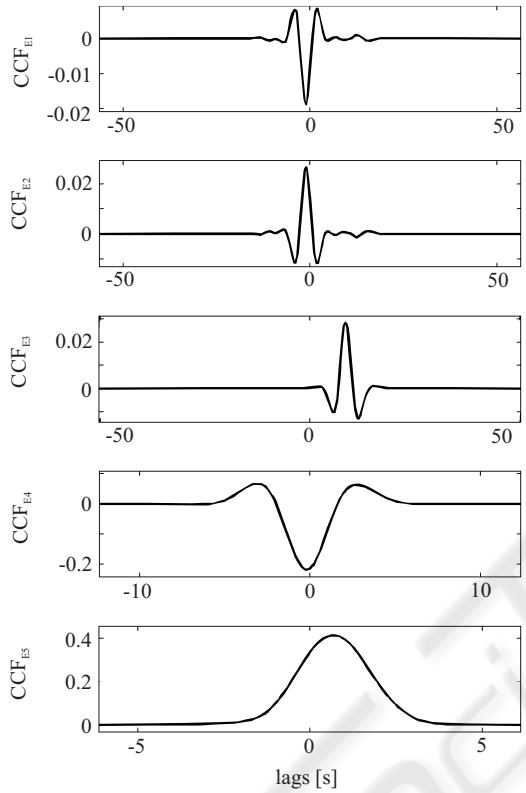

Figure 13: Cross-correlation functions for the parameter settings of Table 1.

Table 2: Symmetry values for parameter settings in Table 1.

parameter settings	symmetry value in %
E1	99.79
E2	99.74
E3	99.43
E4	99.97
E5	99.96

Figure 14 displays the eigenform's cross-correlation functions of another EMG-signal. The eigenforms are based on a pulse detection whose parameters are shown in Table 3. Due to a poorer signal-to-noise ratio, the minimum level value is set to 0.2. Only CCF_{E8}, the CCF for the third parameter set (level value of 0.2, area value equal to 0.7) seems quite symmetric. This assumption is confirmed by a symmetry value $C_{\text{symm}} = 0.9975$ in Table 3.

This means that the eigenforms of the second EMG-signal are more sensitive to variations of the pulse detection's parameters. This may be caused by an incorrect application of the surface sensors, which induces additional noise and deformations. Therefore, the combination of the eigenforms' loadings and the symmetry value indicates the quality of the measurement.

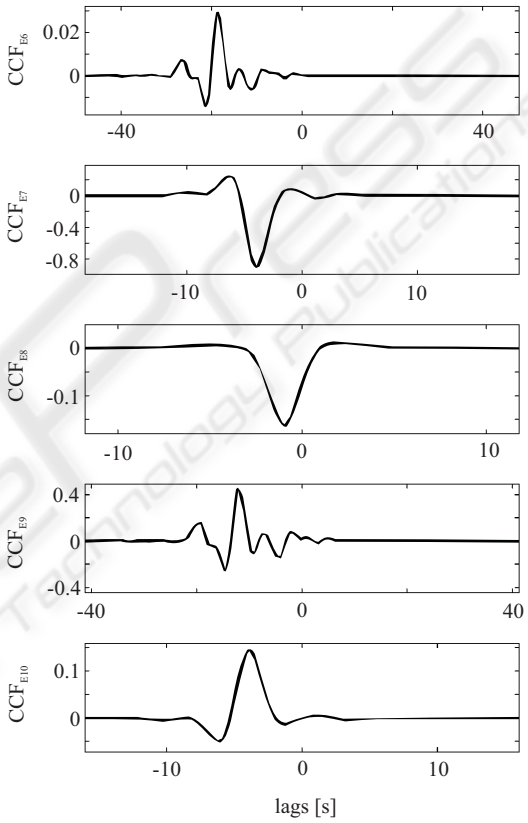

Figure 14: Cross-correlation function of another EMG-signal with parameter settings of Table 3.

Table 3: Symmetry values of the second EMG-signal.

parameter settings	level value	area value	symmetry value in %
E6	0.2	0.1	86.29
E7	0.2	0.4	97.16
E8	0.2	0.7	99.75
E9	0.3	0.1	77.23
E10	0.3	0.4	96.19

4 CONCLUSIONS

The existing methods for the analysis of EMG-signals are not precise enough for a reliable prediction of the point of delivery. The new approach presented in this contribution is based on the distinction between pulses (muscular contraction) and flat line sections during relaxation. A time-frequncy analysis reveals that only the pulses contain relevant information whereas the flat line sections can be neglected. For this reason, a semi-automatic pulse detection is developed. The physician controls the functionality of the pulse detection by adapting two comprehensible parameters, while the time-consuming work of pulse extraction is done automatically. The first parameter, the level value, influences the number of extracted pulses, whereas the second parameter, the area value, determines the length of the pulses. Therefore, the physician integrates his current observations as well as his medical experiences into the pulse detection.

The use of surface electrodes leads to deformations in the individual pulse shapes. In this approach, the pulses extracted by the pulse detection are treated as realisations of a stationary stochastic process. In order to derive a generalized pattern, a stochastic analysis, the Karhunen-Loève-Transform (KLT), is carried out. The KLT is based on the eigenvalue/eigenvector problem of the covariance matrix. While an eigenvector represents a generalised pattern, the corresponding eigenvalue specifies the degree of similarity with regard to the pulse ensemble. Eigenvalue and eigenvector yield to the eigenform. The more dominant the first eigenform is, the better it represents the pulses of the ensemble.

Until now, the mean frequency has been used for the prediction of the point of delivery. Although the pulse detection reduces the frequency deviation significantly, the mean frequency remains sensitive to variations of the pulse detection's parameters because the individual pulses are randomly distorted by conductivity effects. The first eigenform of the KLT is less susceptible to parameter variations. Particular in case of a dominant first eigenform, the mean frequency becomes a reliable criterion.

Furthermore, a new characteristic value is developed: the symmetry value. It is derived from the cross-correlation function of the first eigenforms of the left and right EMG-channel. If the quality of the electromyogram is high, the pulse ensembles of the left and right channel will yield to quite identical eigenforms and a symmetry value close to 100 %. Together with the eigenvalues of the KLT, the symmetry value serves as a criterion for the measurement's reliability.

In the future, the pulse detection combined with the stochastic analysis will be applied on a sufficiently large amount of electromyograms taken from various women during the last period of pregnancy. With these results, the reliability of this new approach as well as the improvement with regards to the present methods will be be quantified.

REFERENCES

Jolliffe, I. T. (2002). *Principal Component Analysis*. Springer, New York, 2nd edition.

Maul, H., Maner, W. L., Olson, G., Saade, G. R., and Garfield, R. E. (2004). Non-invasive transabdominal uterine electromyography correlates with the strength of intrauterine pressure and is predictive of labor and delivery. In *The Journal of Maternal-Fetal and Neonatal Medicine*. Parthenon Publishing.

Mertins, A. (1999). *Signal analysis: wavelets, filter banks, time-frequency transforms and applications*. Wiley, Chichester, 2nd edition.

Oppenheim, A. and Schafer, R. W. (1999). *Discrete-time signal processing*. Prentice Hall, Upper Saddle River, NJ, 2nd edition.

Reicke, L., Kaiser, I., and Kroeger, M. (2006). Identification of the running-state of railway wheelsets. In *ISMA2006, International Conference on Noise & Vibration Engineering*. Katholieke Universiteit Leuven, Department of Mechanical Engineering.